T_2-STORE-T_2 RELAXATION EXCHANGE NMR TO CHARCTERISE EFFECT OF ASPHALTENES ON WETTABILTY DYNAMICS IN SILICEOUS SYSTEMS

Igor Shikhov, Rupeng Li, Ji-Youn Arns, Christoph H. Arns
University of New South Wales, Sydney, Australia

This paper was prepared for presentation at the International Symposium of the Society of Core Analysts held in Vienna, Austria, 27 August – 1 September 2017

ABSTRACT

The asphaltene fraction of crude oils is one of the main factors defining wettability conditions and ultimate oil recovery. At reservoir scale asphaltenes may cause reservoir compartmentalization and at pore scale govern wettability phenomena. To reproduce reservoir conditions, aging in oil is a common step in laboratory core analysis. Oils relevant to the origin of the plugs are the apparent choice for aging, while for outcrop rocks various hydrophobic chemicals and anti-wetting agents or arbitrary oils are often used. We evaluate alteration properties of synthetic oils represented by various proportions of commercially available bitumen, aromatics and alkane for studies requiring wettability alteration.

Low-field NMR relaxation measurements have been applied in the past to characterise the wettability of rocks by introducing an NMR wettability index. However, the latter requires multiple reference measurements at end-point saturation states. NMR correlation techniques have a higher prediction capacity, e.g. T_2-store-T_2 (REXSY) experiment is naturally sensitive to spatial variation of physical properties by detecting diffusion exchange between different environments. It has been applied to study the connectivity of the pore space in aqueous systems such as gypsum, cement pastes, soils, etc. We applied REXSY to study effect of asphaltenes deposition on wettability of siliceous systems. The change of wettability over aging time in different synthetic oils was tracked using T_2 relaxation measurements, providing estimates of aging dynamics useful in designing wettability-related experiments. Quantitative information about fraction of altered surface area and deposition pattern was inferred from combination of T_2 experimental and numerically simulated responses and from T_2-store-T_2 experiments.
Results show that the wettability alteration process is strongly sensitive to both chemical composition of synthetic oils and asphaltenes origin (light or heavy oil). It can be performed in controlled manner to set variety of heterogeneous wetting conditions. Elements of resulting deposition pattern and wetting state of the core were identified using low-field NMR relaxation and relaxation exchange techniques.

INTRODUCTION

Asphaltenes: Understanding their behavior is among the major problems in upstream and downstream petroleum engineering as they may change wettability and create barriers to flow at various scales. Wetting properties of natural rocks motivate studies of

mechanisms governing wettability change, relationships between wettability and rock petrophysical and reservoir properties, detection techniques, and methods allowing restoration and control of wettability change and associated chemo-physics at reservoir conditions. Asphaltenes' dynamics represents a complex process considering their flocculation behavior, interaction with other fluid components and minerals over a broad range of temperature and pressure. On the molecular level asphaltenes dynamics can be well described using Yen-Mullins model [1]. Here we focus mainly on the effect of pore-scale asphaltene-to-solid interaction and their accumulation in rock void space rather than stability/solubility chemistry.

Wettability: a mutual solid-fluid property defined as the tendency of a fluid to spread over or adhere to a solid surface in the presence of other immiscible fluid(s), wettability is one of the main factors governing oil recovery since it controls initial fluids distribution, capillary pressure and relative permeability. It is a multi-scale phenomenon depending on mutual intermolecular interactions between fluids and solids, chemical potential of components, excess of free energy in the solids in contact with fluids (surface energy) and surface roughness (topology). Wetting properties of rocks in context of petroleum engineering are considered qualitatively, ranging from strongly water-wet to strongly oil-wet. These states are often expressed either through contact angle (which is a microscopic property) or more often through one of wettability indices which relate observable change of saturation and saturation history to rock wetting capacity (macroscopic average property), such as Amott [2] and US Bureau of Mines (USBM) methods. The Amott wettability index relates the ratio of spontaneous to forced displacement of oil and water on a -1 to +1 scale. A comprehensive description of these techniques can be found elsewhere, [3]. Alternative approaches include direct measurement of zeta potential [4], various contact angle measurements using e.g. telescope-goniometry [5], Wilhelmy balance method [6].

NMR Wettability Index and Surface Relaxivity Heterogeneity: NMR is widely used for petrophysical characterization of rocks, including applications to wettability [7]: NMR relaxation is sensitive to the wetting state of the rock through surface relaxivity, which lead to the definition of NMR indices correlating very well to standard USBM [8] and Amott [9]. Further improvements were achieved with the aid of numerically modelled NMR responses using simplified pores geometries, e.g. 2D triangular [10]. These models assume homogeneity of surface relaxivity and wettability. The significance of wettability heterogeneity on relative permeability is long known [11]. Effects of surface relaxivity heterogeneity on log mean relaxation time and associated permeability correlations were investigated numerically using simulated NMR relaxation experiments and 3D micro-CT representations of rock and various spatial relaxivity distributions [12]. A systematic experimental study of surface relaxivity heterogeneity on relaxation rates using sand packs altered with ferrihydrite is given in [13]. There is clear proof that variations of wettability of a given mineral constituent of the rock correspond to variations of surface relaxivity. However, it is less obvious how precipitation of asphaltenes following various scenarios (favoring pore topology or mineralogy or combination of both) would affect such interpretation.

Wettability Reversal/Alteration in SCAL (Ageing): Core analysis for the purpose of evaluation of reservoir quality and petrophysical studies requires restoration of core wettability state. This is typically achieved by making a core strongly water-wet using a variety of cleaning procedures and subsequent alteration of the core wettability to some degree of oil wetness. The latter can be achieved either using special hydrophobic chemicals and anti-wetting agents (e.g. dimethyldichlorosilane $Si(CH_3)_2Cl_2$) or using a so-called ageing process – exposure of the rock to crude oil (native to rock origin or arbitrary) at a certain elevated temperature. Where possible, crude oils native to core samples are used. However, in many cases, e.g. for benchmark studies on outcrop rocks or phenomenological studies the selection of oil is arbitrary, which complicates comparison of results. Wettability and asphaltene deposition studies typically involve at least two steps: setting initial conditions of solid (porous) system and alteration of wettability by exposure of solid to long-chained hydrocarbons - ageing at certain conditions (temperature and pressure). In this work we systematically study the effect of two cleaning solvents (light alkane and basic aromatic) as well as the effect of oil composition on strength and rate of wettability alteration.

Distribution and Rate of Asphaltene Deposition: mechanisms and dynamics of asphaltene deposition are of significant importance in upstream and downstream petroleum engineering. At given conditions, asphaltenes likely precipitate on rock surfaces non-uniformly, depending on mineralogy, pore shape, surface roughness, etc. Understanding the influence of these factors will assist in improving multiphase flow models. One apparent effect of asphaltenes deposition is porosity and permeability reduction. There are many techniques and their combinations which have been applied for direct and indirect detection of the deposition process. One work utilised SEM observation and pressure drop in capillary, concluding that submicron asphaltene aggregates are likely responsible for fouling rather than large matured ~0.5 μm aggregates [14]. Other works often rely on various optical microscopy/ photomicrography techniques. Wang *et al.* (2004) [15] investigated deposition rates of asphaltenes mixed with n-alkanes on metallic surfaces in the temperature range of 20 to 60°C. They concluded that governing factors include base crude oil properties, oil/alkane ratio and alkane carbon number. Two base crude oils were used with very similar composition and properties and deposit thickness was measured indirectly: by pressure drop in capillary and by mass balance (asphaltenes in influent and effluent). The thickness of deposits varied between 2 and 70 μm depending on conditions. 3D optical microscopy was applied to investigate the effect of carbon dioxide on asphaltenes deposition at various pressures by detecting size of asphaltene aggregates and glass surface area covered by deposit [16]. Direct or 3D detection of asphaltene deposition processes has an apparent advantage over the indirect or 2D measurements. 3D optical microscopy was applied to measure deposition rate in a glass microchannel as function of pumped volume at a constant and variable flow rate [17]. Experiments were conducted for 4-14 hours at constant temperature 21°C. There was no apparent flow rate dependency on deposition thickness, while fraction and especially type of n-alkane and oil in the mixture changes thickness sometimes significantly, Figure 1 [a,b]. Zhao *et al.*

(2016) [18] studied the impact of asphaltenes precipitation on sandstone during CO_2 flooding using high resolution micro-CT tomography to directly detect deposits. Other examples include a combination of multiple techniques, where micro-CT is used to determine oil and water distribution within pore space, while asphaltene deposition is evaluated using FESEM and optical profilometry providing 3D surface maps [19]. Examination of wetting characteristics of 55 crude oils and pure samples by measuring advancing contact angle values as function of aging time revealed that deposition of surfactants and asphaltenes gradually renders the surface progressively more oil-wet with respect to time as the system ages [20], Figure 1 [c]. Note, both deposition [17] and contact angle time-series data [20] follow very well the logarithmic trend.

Oil Composition and Wettability: Published experimental results show different wettability effects caused by asphaltenes originating from heavy and light oils [21]. This stresses the importance of molecular-level studies targeting the influence of asphaltenes structure. In this study we used natural and synthetic oils containing asphaltenes from light and heavy oils in the various ratios: 1:0, 0.6:0.4, 0.3:0.7 and 0:1. We discuss our observations regarding this effect. The present work focusses on the following aspects relevant to the influence of asphaltenes on rock petrophysical/reservoir properties:

- rate of asphaltenes deposition in sandstone saturated with various synthetic oils after ageing process (after cleaning/re-saturation with n-alkanes),
- rate of wettability change and potential correlation to deposition rate,
- effect of asphaltene deposition and wettability change on NMR T_2 relaxation and T_2-store-T_2 relaxation exchange NMR measurements, characterization of deposition pattern and evaluation of wettability heterogeneity,
- influence of oil composition on aging efficiency.

We aged bead packs and outcrop sandstone with a variety of crude and synthetic oils to investigate the relationship between asphaltene accumulation and wettability change over time depending on oil composition. Wettability change was tracked by measuring NMR relaxation responses. NMR relaxation responses were modelled using random walk simulations with high-resolution micro-CT images as morphological inputs. To interpret results we modelled asphaltene deposition over time using two scenarios: (1) uniform (random) precipitation and accordingly uniform random change of surface relaxivity (with different mean and variance of the affected surface spots); (2) non-uniform, deposition is preferential in crevices defined using radius thresholds on a covering radius transform. Furthermore, for a given ageing time of 14 days depositions were detected directly (within resolution limit) using differential imaging techniques.

EXPERIMENTS

Fluids: In this study we used five synthetic oils composed of various proportions of C170 grade bitumen, toluene, hexadecane and crude oil (Tables 1-3). Asphaltene fraction in these oils varied from 1.6 to 6.6 wt% and resins from 3.4 to 17.4%. All oils are diamagnetic with susceptibility values in a range of -8.0 to -8.5 μSI. Oil 1.b with highest degree of resins and asphaltenes has lowest mean diffusion coefficient of 385 $\mu m^2/s$,

while two oils, 3.d and 4.e, with similarly low resins and asphaltene content (though of different origin) show fastest mean diffusion coefficient of 610 $\mu m^2/s$ (Table 3).

Samples: The rate of asphaltene deposition and wettability change was studied using two porous systems: (1) six borosilicate bead packs plus reference and (2) 36 Bentheimer sandstone core plugs plus two reference plugs. Bead packs we used to test aging capacity of all available oils over the single aging time of 14 days, while 36 sandstone plugs were organized as three sets of 12 plugs aged with three synthetic oils (1.b, 2.c, 3.d) over the 12 time intervals.

We selected borosilicate beads of large size to create bead packs (mean radius r=0.766±0.055 mm) to diminish possible capillary effects on asphaltene precipitation. Beads underwent aging with crude and five different synthetic oils described above (base oil TD, 0.a, 1.b, 2.c, 3.d, 4.e) at room temperature for 4 days following 10 days of ageing at 60°C. Then beads were cleaned in hexane, dried at 60°C for 24 hours and packed in borosilicate bottles (Figure 2 [a-g]). Lastly, bead packs were saturated with n-decane.

We cored 38 Bentheimer sandstone plugs (32~34 mm long and 12.7 mm diameter): two reference cores, never exposed to oils and another 36 were cleaned in methanol, dried and saturated with three types of synthetic oils (1.b, 2.c, 3.d) using the desiccator/vacuum pump setup, 12 samples per each oil type. The average porosity of these plugs is 24.18±0.22%. These three sets are used to measure oil wettability alteration capacity, ageing rate (and cleaning procedure efficiency).

Rock samples fully saturated with oil were held at room temperature for four days and at the end one sample was spared as reference. Then we start ageing at elevated temperature of 60°C following the time schedule shown in Table 4. Accordingly, each sample was aged once for scheduled aging time and then was cleaned in n-hexane at room temperature for six days. Subsequently, cores were dried and saturated with n-decane (in this work water was not used).

MODELLING

To enhance our understanding about the influence of rock topology and morphology (in addition to chemistry) and to evaluate the potential of NMR relaxometry we employed simulated NMR relaxation experiments utilizing a random walk technique on segmented tomographic images [12]: In the pore space, the random walkers can progress towards any one of the 6 possible directions under internal gradient arising from different susceptibilities. The interactions between fluid and solid phases are simulated by assigning relaxivities to interfaces between phases of non-zero hydrogen index. Then we use a numerical CPMG technique to acquire the signals of an ensemble of spin-packets (isochromats) followed by inversion of the resultant magnetization decay.

During the aging process asphaltenes readily deposit in the following two environments: (a) in the high S/V pore space surfaces, pore crevices and kaolinite patches; (b) onto low S/V grain surfaces, likely with much slower rate if any solvent involved. Alternatively, deposition and change of wetness may occur uniformly on all solid surfaces as a thin layer. These scenarios can be expressed through material balance for asphaltenes phase as following: $V_{a,total} = M_a/(\rho_a \varphi_{a'}) = V_{a,agg} + V_{a,surf} = V_{a,agg} + f_a A_s (\delta_a \varphi_a)$, where $V_{a,total}$ – total

volume of precipitated asphaltene, $V_{a,agg}$ – asphaltene accumulations in crevices, $V_{a,surf}$ – asphaltenes attached on the surface, A_s, f_a and δ_a – surface area of solids, fraction covered with asphaltenes and average layer thickness, ρ_a and φ_a – deposit density and porosity. From experiment M_a and A_s are known, ρ_a can also be measured or evaluated based on literature and minimum value of δ_a can be assumed between 1.5 to 5 nm based on modified Yen-Mullins model [1].

To test these two deposition scenarios against observable NMR relaxation data, we mimic these by relabeling a segmented micro-CT image of Bentheimer sandstone. Initially we have three segmented phases: #1 void/pore space; #2 clay patches; #3 solids (quartz and feldspar). Two additional phases corresponding to asphaltene deposition during the aging process are added as following: #4 accumulations in high S/V regions of initially void space performed by relabelling part of phase #1 by thresholding a covering radius field (CRT, the maximum radius of the sphere which can cover the voxel of a phase) [22]. The deposition process on low S/V surfaces is mimicked by creating an imaginary phase #5 at the expense of solid phase #3 (thresholded Euclidean Distance field, EDT – in our case a voxel layer normal to the solid phase surface). This new phase is combined with a uniform random voxelized field so that total fraction of relabelled surface is changed, e.g. as 0%, 50% and 100% (Figure 3 [b-d]). These morphological operations enable us to reproduce a partial or uniform change of surface properties of a solid. Simulated T_2 responses for different wettability/relaxivity scenarios are given in Figure 4, and conceptual and actual spatial relaxivity assignments are given in Figure 3. Main unknown input properties are decane effective diffusion in clay phase and asphaltene patches, diffusion exchange with macro-pores, porosity of asphaltene deposit.

RESULTS

Bead packs: Visual inspection of aged and cleaned bead packs reveals a slight change of beads color after aging in crude oil (Figure 2 [g]); four synthetic oils change beads color to quite similar extent, to medium brown (Figure 2 [c-f]) and aging with oil 4.e resulted in a strongest change of color, to dark brown (Figure 2 [f]). Relaxation time measurements used to calculate the difference of surface relaxivity to n-decane as a function of oil type used for ageing. Relaxation measurements and evaluated surface relaxivity are summarised in Table 5. Oil 4.e demonstrates the strongest increase of relaxivity of aged beads by 40%, oils 1.b, 2.c show significant increase by ~10%, oil 3.d just by 5% and the mixture with the highest fraction of asphaltenes shows the least increase of relaxivity, by 3%. Aging beads in natural crude oil surprisingly decrease relaxivity by 15%, which may be explained by the chemical nature of the deposit (likely wax rather than asphaltenes).

Sandstones: Change in appearance of cores from set 1 (oil 3.d) after aging, cleaning and drying is shown on Figure 5. Cores from this set look much darker (from approx. 17 days of aging, Figure 5 [c]) comparing to cores aged with oils 1.b. and 2.c (all are light to medium brown in color even after 72 days of aging). This has a certain correspondence to the amount of precipitate (Figure 6), but also to precipitate type. The amount of precipitate and degree of color change anti-correlate with regard to the initial amount of

asphaltenes in the oil (which agrees with reported field experience [23]). Surface relaxivity of cores aged with low-asphaltene oil 3.d also increased to a higher extent (from 4.2 μm/s to 9.0 μm/s after 52 days of aging). In comparison, surface relaxivity of plugs aged with high-asphaltene content oil 1.b increased rather little, up to 5.9 μm/s after 52 days (compare to 5.5 μm/s in five days), i.e. remained nearly constant. The main peak of T_2 distributions (Figure 7) moves clearly towards shorter relaxation times and becomes coupled to the short component, the amplitude fraction of which is almost doubled when 3.d oil was used (comparing reference sample and aged for 52 days short-time part of the signal <100 ms increased from 4% to 7%).

The average thickness of deposit and portion of surface it covers can be evaluated if surface area is known. Yan al. (1997) [24] estimated thickness following aging of Berea sandstone of 3.1 nm (for one oil), concluding the presence of a nearly uniform asphaltene monolayer; for another oil the calculated value of 1.7 nm led to the conclusion of a partially covered surface. Similarly, using specific surface area from MICP experiment of 0.5 m^2/g and assuming a minimum layer thickness of 3 nm we can estimate the possibility of uniformly covered grain surfaces: plugs aged with oil 3.d, 2.c and 1.b may reach that state (if no accumulation occurs) in approximately 20, 25 and 50 days respectively based on total precipitate amount, Figure 6 [a]. We can test this estimate by comparing several experimental T_2 distributions, e.g. for samples aged with oil 3.d (BH1.7, BH1.9, BH1.11 aged for 22, 36 and 72 days respectively) with the set of simulated responses where uniform relaxivity was used (Figure 4 [a]). Distributions match is obtained with following relaxivity values (experiment vs simulation): BH1.7: 6.8 vs 5.5 μm/s; BH1.9: 7.8 vs 7.0 μm/s; BH1.11: 10.2 vs 11.0 μm/s; non-aged core: 4.2 vs 4.2 μm/s. Assuming fractional additivity of responses for non-altered and fully altered surfaces, the altered surface fraction is: BH1.7: 15~35%; BH1.9: 40~60%; BH1.11: 90~100%. We can test that finding for the core BH1.9 against simulations performed using 50% of solid surface altered with different relaxivities; experiment expected to match simulated T_2 distribution if 50% of solid surface accept relaxivity 10-11 μm/s. One can see that the experimental distribution overlaps with the simulated curve corresponding to a surface relaxivity of 10 μm/s (Figure 4 [b]). This is rather a solid prediction of the partially altered surface or equally a wetting heterogeneity.

T_2-store-T_2: Similarly to T_2 relaxation, REXSY [25,26] detects the increase of short-time component fraction in total 2D signal amplitude as function of ageing time (peak CC and exchange cross-peaks CB and BC) as well as decrease of the long-time component (peak AA), Figure 9 [b,c]. The evolution of the peak AA over time may be used to track changes of effective surface relaxivity and wettability (calibration to reference sample required, than it recovers relaxivity evaluated from 1D T_2 data within 2-5% difference). More interestingly, based on 2D maps we may suggest certain morphological similarity between responses from kaolinite and asphaltene deposits (Figure 9 [a-c]). Properties of kaolinite in Bentheimer rock are well-known and can be found elsewhere. Comparing the intensity of peaks CC, CB and BC of aged samples to reference and noting the known total amount of deposit, we can evaluate deposit apparent porosity of 0.73 (oil 3.d) and 0.75 (oil 1.b) for samples aged for 22, 36 and 52 days.

DISCUSSION

Our results demonstrate that surface relaxivity of aged sandstone changes with the rate specific to oil chemical composition. Oil with the highest asphaltene content (1.b) demonstrates the least wettability alteration capacity, while oil different from 1.b only in factor 2.5 lower asphaltenes fraction (3.d) much higher alteration strength. In a long aging time (17–72 days) relaxivity changes with time linearly (Figure 6 [b,c]), with the rate ratio 3 : 6 : 1 for oils 3.d, 2.c and 1.b respectively. The highest rate of relaxivity change in sandstone is ten folds slower comparing to published data for the case of flow in capillary, [17], Figure 1 [a,b]. This signifies difference in asphaltenes concentration condition and the impact of a cleaning step. For borosilicate beads aged over 14 days a little difference was found in ageing capacity in three oils of interest (1.b, 2.c and 3.d), with slight preference to the one with highest asphaltene content (10.4, 9.9 and 9.6 μm/s respectively). In our opinion these results evidence that the surface to volume ratio of the aged medium is among the primary factors governing deposition rate and accordingly rate of wettability change. Experimental results of sandstone ageing rate (Figure 6) show that mobility of oil constituents (or bulk-self diffusion coefficient) may be as important as amount of asphaltenes in the oil. Comparing oils 1.b and 2.c with similar asphaltenes content (3.9 % vs 3.4%) we can see that the latter changes wettability/relaxivity 6 times stronger/faster. The higher mobility of oil 2.c together with presence of asphaltenes originated from both light and heavy oils enhanced wettability alteration capacity of the mixture. REXSY technique provides estimate of deposit apparent porosity and together with material balance may be utilized to evaluate deposition pattern.

CONCLUSION

We demonstrated that low-field NMR is suitable to monitor wettability state in time-series experiments. Data show that wettability alteration can be performed in a controlled manner, i.e. by adjusting synthetic oil composition. Experiments demonstrate feasibility of NMR relaxation-exchange technique to identify deposition pattern - fraction deposited as the surface layer and fraction precipitated as aggregate, as well as porosity (packing factor) of the latter. Understanding the dynamics of wettability alteration/restoration in the laboratory improves our ability to reproduce reservoir conditions before performing core tests and aid to ensure representativeness of laboratory data. It also provides pathway for solution of a forward pore-scale wettability problem of unknown spatial distribution and magnitude of surface relaxivity by numerical NMR relaxation experiment.

ACKNOWLEDGEMENTS

CHA acknowledges the Australian Research Council (ARC) for a Future Fellowship and the National Computing Infrastructure for generous allocation of computing time.

REFERENCES

1. Mullins, O.C., ‘The modified Yen model’, *Energy Fuels*, (2010) **24**, 2179.
2. Amott, E., ‘Observations relating to the wettability of porous rock’, *Trans. AIME*, (1959) **216**, 156.
3. Dandekar, A.Y., *Petroleum Reservoir Rock & Fluid Properties*, *CRC Press*, (2013).

4. Bassioni, G. *et al.*, 'Wettability studies using zeta potential measurements', *J. Chem.*, (2015) 743179, 1.
5. Bigelow, W.C. *et al.*, 'Oleophobic monolayers. I. Films adsorbed from solution in non-polar liquids', *Coll. Interface Sci.*, (1946) **1**(6), 513-538.
6. Wihelmy, L.A., 'Über die Abhängigkeit der Kapillaritäts-Constanten des Alkohol von Substanz und Gestallt des benetzten festen Körpers', *Ann. Phys.*, (1863) **119**, 177.
7. Fleury, M. *et al.*, 'Quantitative evaluation of porous media wettability using NMR relaxometry', *Magn. Reson. Imag.*, (2003) **21**, 385.
8. Looyestijn, W. *et al.*, 'Wettability-index determination by nuclear magnetic resonance', *SPE Res. Eval. Eng.*, (2006) **9**(2), 146.
9. Chen, J. *et al.*, 'NMR wettability indices: Effect of OBM on wettability and NMR responses', *J. Petr. Sci. Eng.*, (2006) **52**, 161.
10. Al-Mahrooqi, S.H. *et al.*, 'Pore-scale modelling of NMR relaxation for the characterization of wettability', *J. Petr. Sci. Eng.*, (2006) **52**, 172.
11. Blunt, M.J., 'Effects of heterogeneity and wetting on relative permeability using pore level modeling', *SPEJ*, (1997) **2**(1), 70.
12. Arns, C.H. *et al.*, 'NMR petrophysical predictions on digitized core images', *Petrophys.*, (2007) **48**(3), 202.
13. Keating, K. *et al.*, 'The effect of spatial variation in surface relaxivity on nuclear magnetic resonance relaxation rates', *Geophys.*, (2012) **77**(5) , E365.
14. Hoepfner, M.P. *et al.*, 'A fundamental study of asphaltene deposition', *Energy Fuels*, (2013) **27,** 725.
15. Wang, J. *et al.*, 'Asphaltene deposition on metallic surfaces', *J. Dispers. Sci. Technol.*, (2004) **25**, 287.
16. Zanganeh, P. *et al.*, 'Asphaltene deposition during CO2 injection and pressure depletion: a visual study', *Energy Fuels*, (2012) **26**, 1412.
17. Zhuang Y. *et al.*, 'Three dimensional measurements of asphaltene deposition in a transparent micro-channel', *J. Petr. Sci. Eng.*, (2016) **145**, 77.
18. Zhao, Y. *et al.*, 'Visualization of asphaltene deposition effects on porosity and permeability during CO2 flooding in porous media', *J. Vis., (2016)* **19**, 603.
19. Kumar, M. *et al.*, 'Patterned wettability of oil and water in porous media', *Langmuir*, (2010) **26**, 4036.
20. Treiber, L.E. *et al.*, 'A laboratory evaluation of wettability of fifty oil-producing reservoirs', *SPE J*, (1972) **12**(6), 531.
21. Dashti, H. *et al.*, 'The comparison between heavy and light oil asphaltene deposition during pressure depletion and CO2 injection at reservoir condition, a visual laboratory study', *Chemeca Conf.*, (2013) 30298, *Brisbane, Australia.*
22. Arns, C.H. *et al.*, 'Cross-property correlations and permeability estimation in sandstone', *Phys. Rev. E*, (2005) **72**:046304:1.
23. de Boer, R. *et al.*, 'Screening of crude oils for asphalt precipitation: Theory, practice, and the selection of inhibitors', *SPE Prod. & Fac.*, (1995) **10**(1), 55.
24. Yan, J. *et al.*, 'Wettability changes induced by adsorption of asphaltenes', *SPE Prod. & Fac*., (1997) **12**(4), 259.
25. Lee, J.-H. *et al.*, 'Two-dimensional inverse Laplace transform NMR: Altered relaxation times allow detection of exchange correlation', *J. Am. Ceram. Soc.*, (1993) **115**, 7761.
26. Washburn, K.E. *et al.*, 'Tracking pore to pore exchange using relaxation exchange spectroscopy', *Phys. Rev. Let.*, (2006) **97**, 175502:1.

TABLES AND FIGURES

Table 1. Component of mixtures representing five synthetic oils.

Hydrocarbon	Bitumen, wt.%	Crude oil, wt.%	n-$C_{16}H_{34}$, wt.%	Toluene, wt.%
Synth. Oil "0.a"	41.7	0.0	0.0	58.3
Synth. Oil "1.b"	25.0	0.0	40.0	35.0
Synth. Oil "2.c"	15.0	30.0	15.0	40.0
Synth. Oil "3.d"	10.0	0.0	50.0	40.0
Synth. Oil "4.e"	5.0	30.0	30.0	35.0

Table 2. SARA analysis of base hydrocarbons and mixtures.

Hydrocarbon	Saturates, %	Aromatics, %	Resins, %	Asphaltenes, %	Volatiles + LOC
Crude oil	38.40	5.60	4.20	3.49	48.30
Bitumen C170	12.90	28.80	41.70	15.72	0.90
Synth. Oil "0.a"	5.38	70.31	17.39	6.56	0.38
Synth. Oil "1.b"	43.23	42.20	10.43	3.93	0.23
Synth. Oil "2.c"	28.46	46.00	7.52	3.41	14.63
Synth. Oil "3.d"	51.29	42.88	4.17	1.57	0.09
Synth. Oil "4.e"	42.17	38.12	3.35	1.83	14.54

Table 3. Physical properties, Total Acid Number, Total Base Number and magnetic susceptibility.

Hydrocarbon	Density, /cc	Viscosity, cP	D, μm²/s	AN, mg KOH/g	BN, mg KOH/g	χv, μSI
n-hexadecane	0.7713	3.25	402	-	-	-8.08
n-decane	0.7277	0.89	1328	-	-	-7.64
Toluene	0.8625	0.60	2163	-	-	-7.57
Crude oil	0.8134	16.41	198	1.19	0.66	-8.56
Bitumen C170	1.0304	-	-	1.90	3.80	-9.76
Synth. Oil "0.a"	0.9325	6.04	478	0.79	1.58	-8.48
Synth. Oil "1.b"	0.8792	3.61	385	2.37	1.00	-8.32
Synth. Oil "2.c"	0.8529	2.42	510	1.14	0.78	-8.27
Synth. Oil "3.d"	0.8240	1.78	610	1.63	0.32	-8.04
Synth. Oil "4.e"	0.8235	1.85	607	1.40	0.40	-8.22

Table 4. Ageing schedule (at 60°C).

Step/sample No	1	2	3	4	5	6	7	8	9	10	11	12
Time step, d*t* [days]	0	1.5	2	2.5	3	4	5	6	8	16	24	28
Total aging time, *t* [days]	0	1.5	3.5	6	9	13	18	24	32	48	72	100

* All samples were initially aged at room temperature of 22°C for four days (our initial condition).

Table 5. Average weight gain and calculated average deposit thickness

Beadpack sample	Ref 1	Ref 2	0.a	1.b	2.c	3.d	4.e	TD
N beads, estimated [pcs]	5114	5260	5059	5135	5092	5107	5076	5006
S/V calculated [μm⁻¹]	0.0068	0.0070	0.0069	0.0072	0.0070	0.0070	0.0071	0.0070
S/V evaluated 3/*r* [μm⁻¹]	0.0255	0.0255	0.0255	0.0255	0.0255	0.0255	0.0255	0.0255
Relaxition time, T_2 [ms]	1028.9	1049.6	1023.1	1007.6	1010.4	1011.8	1026.7	1064.4
ρ_2 (*e*) effective [μm/s]	3.41	3.50	3.56	3.94	3.73	3.63	4.17	2.99
ρ_2 evaluated [μm/s]	9.01	9.23	9.39	10.38	9.85	9.57	11.01	7.89

Calculated S/V used known weight of beads; Evaluated S/V used surface area of inscribed spheres.

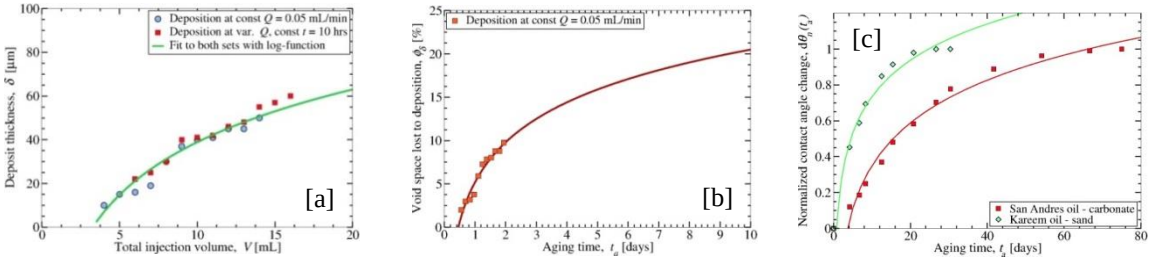

Figure 1. **[a]** Growth of asphaltenes in a capillary tube at constant flow rate over 48 hrs / variable rate at constant time 10 hrs, [17]. **[b]** Constant flow rate data is replotted as normalized void space loss over time. **[c]** Contact angle change during aging in native crude oils for two reservoir rocks excerpted from [20]: re-plotted as normalized contact angle change $d\theta_n(t_a)$. All data [a-c] fitted with log-function: $A + B\ ln\ (t)$.

Figure 2. Reference 20 cc borosilicate beadpack **[a]** and beadpacks aged 14 days in different natural and synthetic oils (dried): **[b]** oil 0.a; **[c]** oil 1.b; **[d]** oil 2.c; **[e]** oil 3.d; **[f]** oil 4.e; **[g]** crude oil.

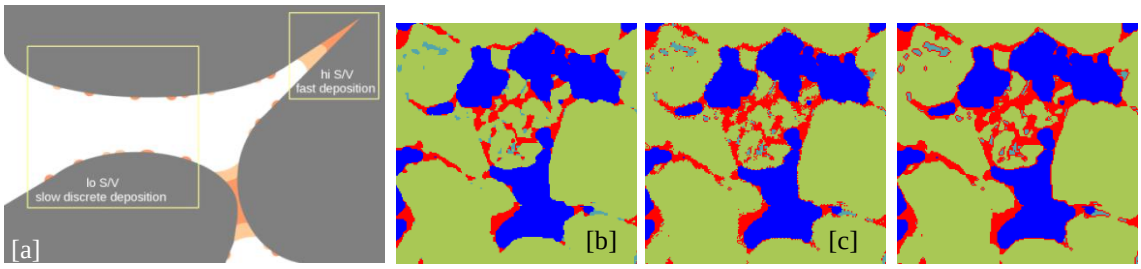

Figure 3. **[a]** Concept of two competing deposition processes, rates of which governed by local surface-to-pore ratio. **[b-d]** The slice through the segmented Bentheimer sandstone µ-CT image altered using morphological transforms to create an additional phase following three deposition scenarios: **[b]** deposition occurs in the pore crevices only (high S/V); **[c]** same as [a], in addition 50% of grain surface is randomly altered (no volume assigned); **[d]** whole surface is uniformly altered.

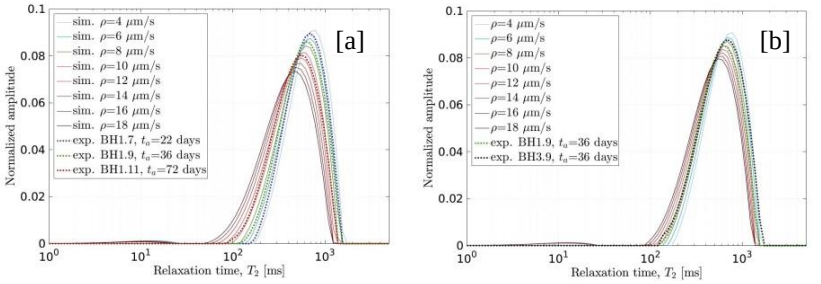

Figure 4. Simulated T_2 distributions of decane-saturated Bentheimer for two deposition scenarios: **[a]** surfaces are altered uniformly. **[b]** deposition in the crevices and 50% of grain surface is altered.

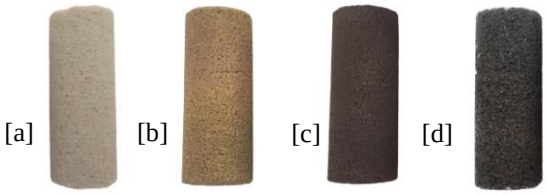

Figure 5. Bentheimer cores **[a]** non-aged reference; aged in synthetic oil 3.d over **[b]** 10 days; **[c]** over 22 days; **[d]** 36 days. Cores were pictured after cleaning in n-hexane and drying.

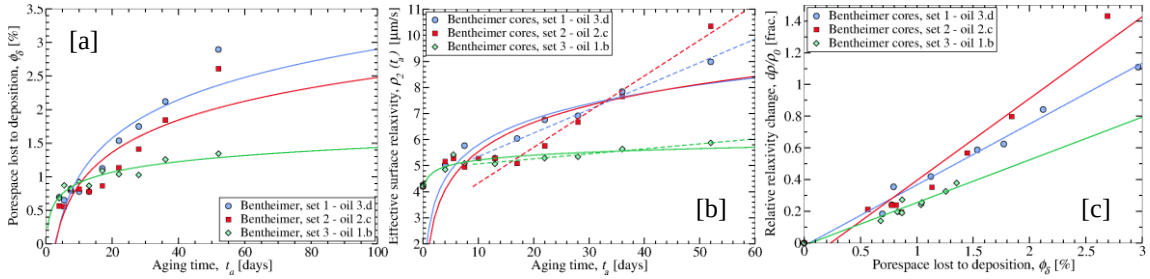

Figure 6. **[a]** Porespace fraction of cores lost to precipitate deposition φ_δ (from weight gain) for synthetic oils 1.a, 2.c and 3.d. **[b]** Change of surface relaxivity over aging time $\rho_2(t_a)$. **[c]** Porespace fraction lost to deposition plotted vs normalized relaxivity change for three sets of cores aged up to 52 days.

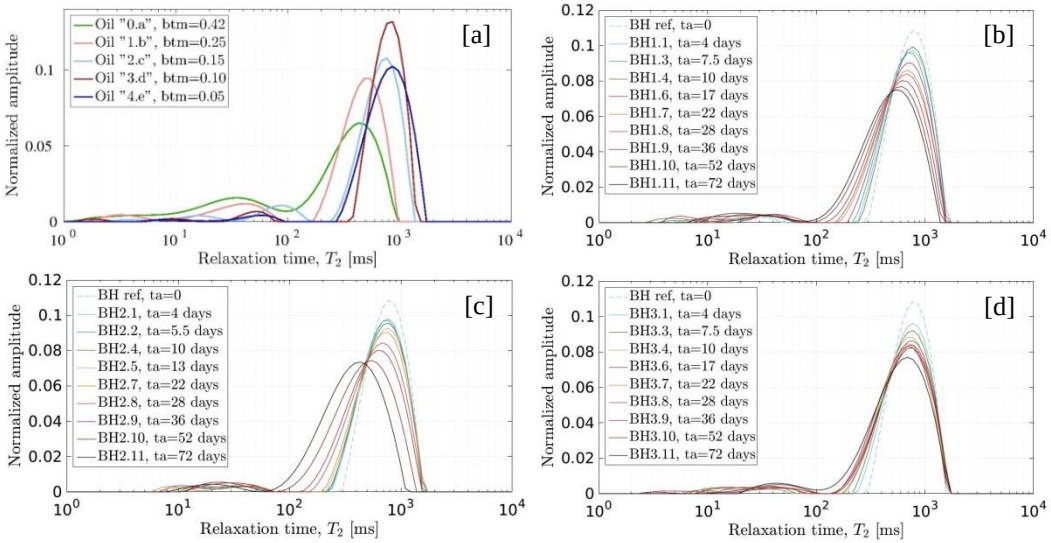

Figure 7. T_2 distributions of **[a]** synthetic oils mixed with different proportions of bitumen (Table 1-3); Bentheimer plugs aged over different time, up to 72 days in three synthetic oils: **[b]** oil 3.d (plugs BH 1.1-1.11); **[c]** oil 2.c (plugs BH 2.1-2.11); **[d]** oil 1.b (plugs BH 3.1-3.11).

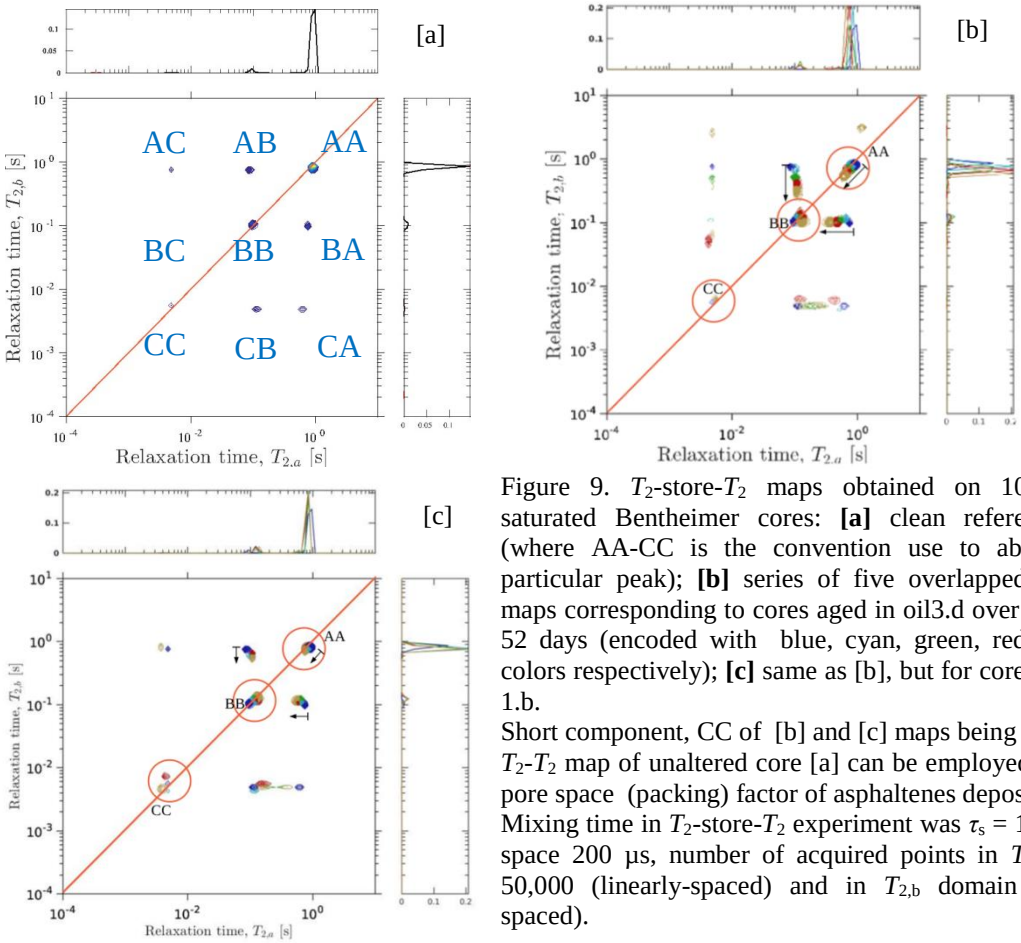

Figure 9. T_2-store-T_2 maps obtained on 100% decane saturated Bentheimer cores: **[a]** clean reference sample (where AA-CC is the convention use to abbreviate the particular peak); **[b]** series of five overlapped T_2-store-T_2 maps corresponding to cores aged in oil3.d over 0, 4, 22, 36, 52 days (encoded with blue, cyan, green, red and brown colors respectively); **[c]** same as [b], but for cores aged in oil 1.b.

Short component, CC of [b] and [c] maps being calibrated to T_2-T_2 map of unaltered core [a] can be employed to evaluate pore space (packing) factor of asphaltenes deposits.

Mixing time in T_2-store-T_2 experiment was τ_s = 100 ms, echo space 200 µs, number of acquired points in $T_{2,a}$ domain - 50,000 (linearly-spaced) and in $T_{2,b}$ domain - 80 (log-spaced).